

## First-Principles Structures and Stabilities of $\text{Al}_N^+$ ( $N = 46\text{--}62$ ) Clusters

Andrés Aguado\* and José M. López

*Departamento de Física Teórica, Universidad de Valladolid, Valladolid 47011, Spain*

*Received: May 17, 2006; In Final Form: June 26, 2006*

We present plausible candidates for the global minimum structures of  $\text{Al}_N^+$  ( $N = 46\text{--}62$ ) cluster ions, determined by pseudopotential density functional theory static calculations under the spin-polarized generalized gradient approximation. Our calculations provide a first important step toward the rationalization of recent calorimetric experiments on the meltinglike transition of  $\text{Al}_N^+$ . Most clusters with  $N \geq 48$  clearly adopt fragments of the face-centered-cubic (fcc) crystalline lattice, although with significant distortions and a substantial proportion of defects in some cases. Another important driving force for stabilization comes from (111)-like surfaces, as the clusters often prefer to adopt less compact structures in order to keep the proportion of (100)-like surfaces at a minimum level.  $\text{Al}_{46}^+$  and  $\text{Al}_{47}^+$  adopt rather disordered structures instead. We find indications of enhanced stabilities for  $N = 51, 57$ , and  $61$  and of a substantial structural change between  $\text{Al}_{55}^+$  and  $\text{Al}_{56}^+$ . These features correlate, albeit qualitatively, with the experimental observations.

The finite system analogue of the first-order bulk melting transition has now been theoretically studied many times in simulations of cluster melting. These studies reveal, for example, that cluster melting does not proceed abruptly but gradually over a range of energies and that premelting transitions such as surface melting or isomerizations between different solid forms may precede the main transition to the liquid state. Experimental determinations of melting points in clusters have been much more scarce and have appeared more recently. They provide fundamental pieces of information which should be contrasted with the theoretical predictions. Breaux et al.<sup>1</sup> have measured caloric curves for  $\text{Al}_{49}^+ \text{--} \text{Al}_{63}^+$  clusters and identified several intriguing features: local maxima in the latent heat and entropy of fusion appear for  $N = 51, 57$ , and  $61$ , and a substantial drop in the melting temperature starts at  $N = 56$ . Also, premelting features are of the appropriate nature as to be observed in the caloric curves only for  $\text{Al}_{51}^+$  and  $\text{Al}_{52}^+$ . Obtaining some physical insight into these very interesting questions would require the efficient simulation (by either Monte Carlo or molecular dynamics techniques) of the corresponding melting processes on a computer, which in turn requires a model of the atomic interactions with two main qualifications: it must be accurate (in order to generate a chemically accurate potential energy surface (PES)), and its evaluation must be cheap (in order to sample the PES efficiently and obtain meaningful statistical averages). Both requirements, although often confronted, are equally important.

Despite some previous theoretical efforts,<sup>2–16</sup> no definite structural assignment exists yet for Al clusters in this size range. Parametrized potential models predict an icosahedral,<sup>7–11</sup> polytetrahedral,<sup>11,12</sup> or other low-symmetry<sup>13</sup> growing pattern for aluminum clusters over a wide size range. Initial ab initio calculations focused only on smaller sizes<sup>4</sup> or on  $\text{Al}_{55}$ : Cheng

et al.<sup>2</sup> found the cuboctahedron to be more stable than the icosahedron from structural relaxations restricted by the point group symmetry; Ahlrichs and Elliott<sup>5</sup> found that the truncated decahedron has a lower energy than either the icosahedron or cuboctahedron, again from restricted relaxations; Yi et al.<sup>3</sup> found a significantly distorted icosahedron to lie lower in energy if a full geometry relaxation is allowed; Akola et al.<sup>6</sup> found octahedral structures to be more stable for  $\text{Al}_{52}$ ,  $\text{Al}_{54}$ , and  $\text{Al}_{55}$ . The most stable close-packed structures (with a consideration of stacking faults) of  $\text{Al}_N$  with  $N$  up to 110 were investigated by Manninen et al.<sup>14,15</sup> through both pairwise and tight-binding (TB) potentials. Finally, a genetic algorithm search of the global minimum structures of  $\text{Al}_N$  ( $N \leq 23$ ), based also on the TB model, has been performed recently by Chuang et al.<sup>16</sup> It is evident that the ab initio information is incomplete in the size range of interest to this paper and that there is no consensus between different theoretical methods. For example, if icosahedral and/or polytetrahedral structures are not adopted by  $\text{Al}_N$  clusters in this size range (as the scarce ab initio calculations indicate), then all of the  $\text{Al}_N$  melting simulations performed up to now<sup>8–11</sup> are unrealistic. In fact, the bad agreement between the model potential and experimental melting properties led Noya et al.<sup>11</sup> to conclude that  $\text{Al}_N$  ( $49 \leq N \leq 62$ ) clusters should adopt some other structure. Extensive ab initio calculations in the size range relevant to the experiments of Breaux et al.<sup>1</sup> are thus both timely and pertinent. Our main goal in this letter is to employ state-of-the-art first-principles techniques to locate candidate ground state (GS) structures of  $\text{Al}_N^+$  ( $46 \leq N \leq 62$ ), providing thus a first step toward the rationalization of the experimental results.

Unfortunately, employment of unbiased search methods (such as genetic<sup>16</sup> or basin hopping<sup>11,12</sup> algorithms) in conjunction with an ab initio evaluation of energies is still impractical. Our approach in this letter has been to optimize, with a conjugate gradients method, a very large set of initial structures (more than 100 for each size). The initial structures are the following:

\* To whom correspondence should be addressed. E-mail: aguado@metodos.fam.cie.uva.es.

(1) all those reported in the Cambridge Cluster Database (CCDB),<sup>17</sup> that is, not only those obtained from a potential representing aluminum but many others obtained from different interaction models<sup>18–23</sup> (note that the normal approach in many studies, which consists of optimizing ab initio a subset of structures initially generated with just one potential model, would not be useful in this case if the Al potentials are not accurate for clusters, as we will show to be the case); (2) the close-packed structures optimized by Manninen et al.;<sup>14,15</sup> (3) all those obtained from (1) and (2) by adding and/or removing atoms from many inequivalent sites, fully relaxing the structures after each addition/removal; (4) many structures obtained from (2) by changing the stacking fault (SF) sequences; (5) all those obtained from (1) + (2) + (3) + (4) by compressing and/or expanding all interatomic distances with respect to the average equilibrium distance and also by introducing small random initial displacements whenever the initial structure has a high symmetry; (6) high-symmetry icosahedral, decahedral, and cuboctahedral structures built by hand; (7) analysis of the structural trends thus obtained sometimes allowed the manual generation of competitive isomers. This procedure is quite systematic and represents an intensive (and somewhat painful, due to steps 3, 4, and 7 above) effort to locate better candidate structures. Nevertheless, we stress it does not guarantee that one will locate the correct GS isomer for each size, especially if its structure is very different from those taken here as initial reasonable guesses. The important point is that we are considering a great variety of structures including several icosahedral, decahedral, close-packed, and disordered motifs, and the results will be very useful in analyzing structural trends, at the very least. Moreover, we feel reasonably confident that, within the structural families tried, no other isomers with a substantially lower energy exist. We succeed to improve all the structures found previously by other researchers, and an analysis of the results shows some partial agreement with experimental observations, which gives further support to the adopted strategy.

We employ the SIESTA code,<sup>24</sup> which is a self-consistent Kohn–Sham density functional theory (KS-DFT) method employing standard norm-conserving pseudopotentials<sup>25</sup> in their fully nonlocal form<sup>26</sup> and a flexible linear combination of atomic orbitals (LCAO) basis set.<sup>27</sup> Exchange and correlation (XC) effects are treated within the spin-polarized generalized gradient approximation (GGA) of Perdew, Burke, and Ernzerhof.<sup>28</sup> The basis set includes two basis functions per angular momentum channel plus one polarization orbital (DZP in the notation of ref 24), and the energy shift parameter<sup>24</sup> was kept to a value of 20 meV. The fineness of the real space grid employed to calculate Hartree and XC terms is measured by the maximum kinetic energy of the plane waves that can be represented in the grid without aliasing: a value of 100 Ry is found to give converged results. A smearing of the electron energy levels corresponding to a temperature of 100 K was applied to help convergence. A cubic supercell with an edge length of 27 Å was employed, which is sufficient to avoid interaction between cluster periodic replicas. A critical assessment of the adopted methodology was performed by explicit comparison of the results obtained for small  $\text{Al}_N$  clusters ( $N = 4, 6, 7, 13, 14$ ) with those obtained in previous studies from a variety of ab initio approaches of similar and higher quality. This material is offered in the Supporting Information.

Figures 1 and 2 show the lowest-energy structures (the main result from our study), while Figure 3 shows a selection of some other structures with competitive energy. Excepting  $\text{Al}_{46}^+$  and  $\text{Al}_{47}^+$ , which adopt rather disordered, low-symmetry structures,

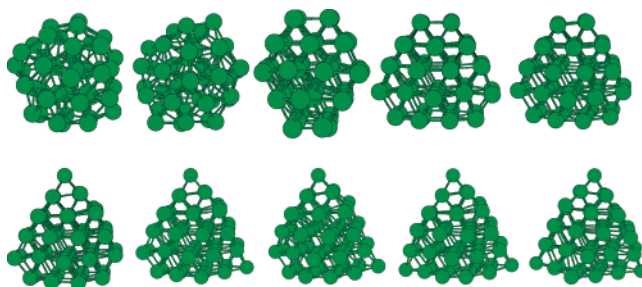


**Figure 1.** Visual representation of the lowest-energy isomers for  $\text{Al}_{46}^+ - \text{Al}_{55}^+$ , ordered from the upper left to the lower right corner. The  $\text{Al}_{55}^+$  isomer has the same energy as that shown in Figure 2, within the accuracy of the calculations.

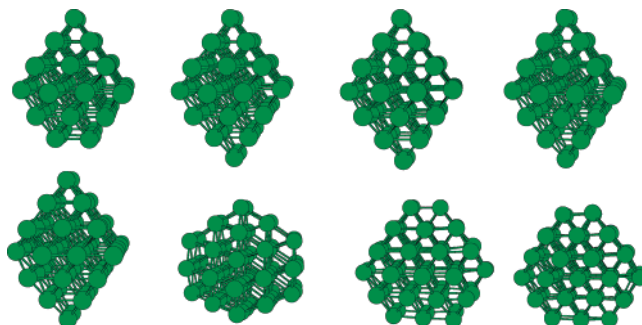


**Figure 2.** Visual representation of the lowest-energy isomers for  $\text{Al}_{55}^+ - \text{Al}_{62}^+$ , ordered from the upper left to the lower right corner. The  $\text{Al}_{55}^+$  isomer has the same energy as that shown in Figure 1, within the accuracy of the calculations.

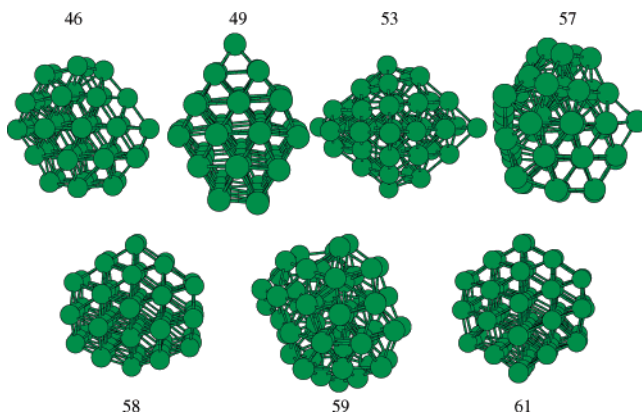


**Figure 3.** Some other isomers which are especially stable, many of them showing distorted decahedral environments.  $\text{Al}_{53}^+$  is a distorted pentagonal bipyramid with a missing vertex.

and  $\text{Al}_{60}^+$ , which shows some remnants of decahedral order, all  $\text{Al}_N^+$  clusters adopt structures based on crystalline face-centered-cubic (fcc)-like close packing. Most often, these structures show substantial distortions and/or defects such as SFs. All clusters show a very small proportion of (100)-like “square” faces and rearrange themselves to expose a maximum amount of (111) close-packed faces. These two features, namely, a tendency toward close-packed structures with a high proportion of (111) faces, summarize the main structural trends. The high preference for (111) surfaces is exemplified by the  $\text{Al}_{53}^+$  isomer shown in Figure 3: it is a distorted two-shell pentagonal bipyramid missing one of the five equatorial vertex atoms, and it represents an isomer with competitive energy in the size range  $N = 50 - 54$ . It is the limit of a decahedron in which the square (100) faces have disappeared. Although it is much less compact than structures based on the 55-atom Ino decahedron or cuboctahedron, it is much more stable.

The structural trends may be analyzed further. Starting with  $\text{Al}_{49}^+$ , a family of similar structures appear which constitute the GS isomers up to  $N = 55$ . All of these structures are built not only by adding an atom to the cluster size immediately below, but some rearrangements of SFs also occur.  $\text{Al}_{55}^+$  no longer has appropriate sites for binding of an additional atom, and another structure emerges beyond  $N = 55$ . This structure is formed by intermixing three half-octahedra (square pyramids) at angles of  $120^\circ$ , as can be easily appreciated from Figure 1. The square faces of these half-octahedra are shared at the cluster center and thus are not exposed to the surface. The several SFs running through the structures are very important in their stabilization. A new structural family covers the range  $N = 55$ –59 (the two  $\text{Al}_{55}^+$  isomers are degenerate within the accuracy of our calculation, with their energy difference being smaller than 0.1 meV/atom):  $\text{Al}_{58}^+$  can be obtained from a 79-atom truncated octahedron by peeling off two neighboring triangular faces. The symmetry of these clusters is thus perfectly octahedral, and they contain no SFs.  $\text{Al}_{61}^+$  and  $\text{Al}_{62}^+$  are again based on close packing but possess a different geometrical shape. Note that experimental mass spectra are consistent with octahedral symmetry for clusters of more than 200 atoms.<sup>29</sup> Here, we find octahedral clusters to be stable for some sizes in the range  $N = 55$ –62.

A comparison to model potential results is quite interesting. It reveals that structures generated with the Gupta and glue Al models<sup>11,12</sup> lie very high in energy, and it can be assessed indeed that these Al potentials are the least representative of real atomic interactions in Al clusters. Therefore, it turns out to be a good idea, in order to efficiently sample the PES by ab initio methods, to feed the first-principles calculations with structures obtained from many different models of interactions, as we do in the present work. The extensive sampling of different model PESs made publicly available at the CCDB<sup>17</sup> is obviously useful in this respect, as some of the identified structural patterns are probably representative of the approximate behavior of a real system, even if this system is not the intended one. For example, we have found that the Gupta potentials parametrized to reproduce atomic interactions in Zn and Cd clusters,<sup>21</sup> or the 10-8 Sutton–Chen (SC10-8) potential<sup>19</sup> (which is assumed to be good for Au and Pt clusters), produce structures which are highly competitive for Al clusters (some of the structures in Figure 3 are based on these potentials). The  $\text{Al}_{55}^+$  isomer shown in Figure 2 is exactly the same as the SC10-8 global minimum. All GS structures found in this work improve over the GS structures found with potential models.

Compared to the TB-potential calculations of Manninen et al.,<sup>14,15</sup> our results show on average a different preference for the formation of SFs. For example, our GS structures for  $N = 48, 59, 60$ , and  $62$  are the best fcc-like structures without SFs found by Manninen et al., but for all of these sizes, they found a lower energy isomer containing SFs. On the contrary, our GS structures for  $N = 52$ –55 contain a significant proportion of SFs while the TB-potential minima of Manninen et al. are pure fcc clusters. For almost all sizes, we are able to identify better fcc-like structures (with or without SFs). It therefore seems that the TB potential is not accurate enough to describe the complex energetics associated with stacking faults. Finally, a comparison with the only unbiased ab initio calculations we are aware of<sup>6</sup> shows agreement with the octahedral  $\text{Al}_{55}^+$  structure shown in Figure 2, but our GS structures for  $\text{Al}_{52}^+$  and  $\text{Al}_{54}^+$  have a lower energy than those proposed by Akola et al.<sup>6</sup>

Figure 4 shows three different measures of cluster stability, namely, the binding energy per atom, the evaporation energy,

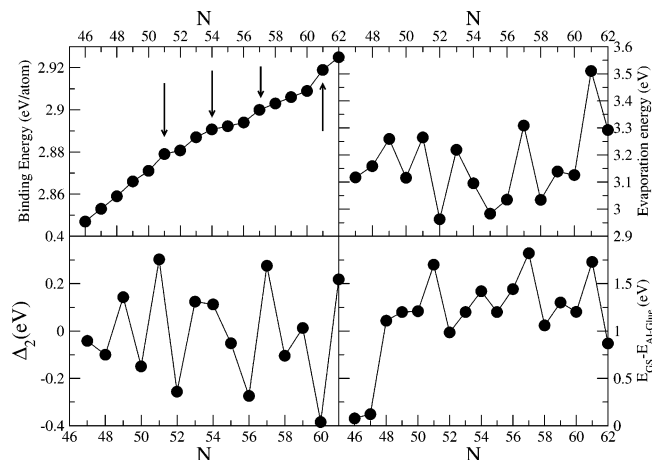


**Figure 4.** Binding energy per atom (upper left), evaporation energy (upper right), second energy difference (lower left), and energy difference between the GS and disordered isomers predicted by the glue model (lower right) as a function of the number of atoms,  $N$ . The arrows point to the sizes with enhanced stability according to the binding energy. Sizes of  $N = 51, 57$ , and  $61$  show enhanced stability in all measures, and  $\text{Al}_{54}^+$  also shows some enhanced stability according to some measures.

and the second energy difference,  $\Delta_2(N) = E(N+1) + E(N-1) - 2E(N)$ . Each quantity refers to a different stability measure, and none of them should be directly related in principle to the latent heats determined in the melting experiments.<sup>1</sup> Nevertheless, sizes of  $N = 51, 57$ , and  $61$  (for which latent heat local maxima are observed) are the ones showing enhanced stability for all three different measures. An undesirable feature of these stability measures is that they show (mostly  $\Delta_2(N)$  and the evaporation energies) a substantial odd–even alternation typical of metal clusters. Odd–even alternation effects are expected to be smoothed out in the evaluation of the latent heats if they persist in the liquid cluster. To have some indirect confirmation of this possibility, we have plotted (not explicitly shown) the  $\Delta_2(N)$  curve for the isomers obtained from the Al glue potential.<sup>12</sup> This potential generates quite disordered polytetrahedral structures except for  $N = 54$  and  $55$ , and their melting curves<sup>11</sup> do not show significant latent heats because the solid and liquid structures are so similar.<sup>30</sup> Being good representatives of the structures sampled in the liquid phase, we observe that the odd–even oscillations clearly persist. In the lower right panel of Figure 4, we show the energy difference between the GS and the glue model structures (for  $N = 54$  and  $55$ , we do not use the icosahedral but the best polytetrahedral structures obtained by adding or removing atoms from the glue model isomers of  $\text{Al}_{53}^+$  and  $\text{Al}_{56}^+$ ). This is in our opinion the most appropriate comparison with the size variation of experimental latent heats that can be done with only static calculations. Regarding the size variation of melting points, we notice that a strong depression is observed in the experiments at  $N = 56$ <sup>1</sup> and attributed to a possible structural change. This is precisely what we observe. Even if two  $\text{Al}_{55}^+$  isomers have essentially the same energy, the isomer of Figure 1 will most probably be favored at high temperatures because, being much more disordered (the distribution of interatomic distances, for example, is much wider than that for the isomer in Figure 2), it will have a lower free energy. To get some support for this hypothesis, we have calculated the normal mode vibrational frequencies of those two  $\text{Al}_{55}^+$  isomers by explicitly evaluating and diagonalizing the force constant matrix. The geometric mean vibrational frequencies are 202 and 206  $\text{cm}^{-1}$  for the  $\text{Al}_{55}^+$  isomer shown in Figures 1 and 2, respectively. These are very similar because



both isomers are based on fcc packing but predict that the isomer of Figure 1 will be favored at high  $T$ , according to the harmonic approximation.<sup>33,34</sup> Thus, the structural change relevant to melting is predicted at  $N = 56$  in this work. Although explicit simulations of melting will be needed in order to confirm full agreement with experiment, the results presented here are the first ones to provide a partial explanation and theoretical support for the calorimetric experiments of Breaux et al.<sup>1</sup>

To conclude, our calculations are important for several reasons: (1) They stress that atomic interactions in Al clusters are not accurately represented by the presently available parametrized potential models and that the full power of first-principles methods must be employed in order to obtain realistic structural trends. In this respect, the situation is substantially more complex than in the case of Na clusters, which are reasonably represented by simpler models.<sup>31,32</sup> (2) As an ergodic sampling of the PES (which is needed in meaningful simulations of cluster melting) is not presently affordable with the computationally expensive ab initio methods, the present results should provide an extensive database for parametrization of simpler models of atomic interactions. Of course, it would be desirable to enlarge this database with some disordered isomers if the energy model is to be used in computer simulations of the melting process. It is our opinion that this feedback procedure (remember that our refinement of structural trends in Al clusters has been in turn guided by previous model calculations) is very convenient in order to extract accurate thermal properties in clusters, and we will consider such a strategy in our future research on Al clusters. (3) The substantial odd–even oscillations observed suggest that electronic effects might still be important for Al clusters of this size. We are also undertaking similar calculations on neutrals and cluster anions in order to check if the charge state can affect structure and therefore the melting properties. (4) Finally, our zero-temperature results, when properly interpreted, show partial agreement with the calorimetric experiments of Breaux et al.<sup>1</sup> and thus provide some hope that theoretical simulations might be able to interpret and explain those experiments.

**Acknowledgment.** This work was supported by the EU-FEDER Program and Ministerio de Educación y Ciencia (MAT2005-03415) and the “Ramón y Cajal” program.

**Supporting Information Available:** An explicit comparison between the DFT results generated with the SIESTA code and those obtained from other ab initio previous studies for aluminum clusters in the small size regime ( $Al_N$ ,  $N = 4, 6, 7,$

13, 14), together with a comparison of the SIESTA results obtained from the two exchange-correlation approximations most frequently employed: LDA and GGA. These comparisons serve to validate the methodology adopted in this paper. This material is available free of charge via the Internet at <http://pubs.acs.org>.

## References and Notes

- (1) Breaux, G. A.; Neal, C. M.; Cao, B.; Jarrold, M. F. *Phys. Rev. Lett.* **2005**, *94*, 173401.
- (2) Cheng, H. P.; Berry, R. S.; Whetten, R. L. *Phys. Rev. B* **1991**, *43*, 10647.
- (3) Yi, J.; Oh, D.; Bernholc, J. *Phys. Rev. Lett.* **1991**, *67*, 1594.
- (4) Akola, J.; Häkkinen, H.; Manninen, M. *Phys. Rev. B* **1998**, *58*, 3601.
- (5) Ahlrichs, R.; Elliott, S. D. *Phys. Chem. Chem. Phys.* **1999**, *1*, 13.
- (6) Akola, J.; Manninen, M.; Häkkinen, H.; Landman, U.; Li, X.; Wang, L. *Phys. Rev. B* **2000**, *62*, 13216.
- (7) Sun, D. Y.; Gong, X. G. *Phys. Rev. B* **1998**, *57*, 4730.
- (8) Jellinek, J.; Goldberg, A. *J. Chem. Phys.* **2000**, *113*, 2570.
- (9) Werner, R. *Eur. Phys. J. B* **2005**, *43*, 47.
- (10) Alavi, S.; Thompson, D. L. *J. Phys. Chem. A* **2006**, *110*, 1518.
- (11) Noya, E. G.; Doye, J. P. K.; Calvo, F. *Phys. Rev. B* **2006**, *73*, 125407.
- (12) Doye, J. P. K. *J. Chem. Phys.* **2003**, *119*, 1136.
- (13) Joswig, J.; Springborg, M. *Phys. Rev. B* **2003**, *68*, 085408.
- (14) Manninen, K.; Manninen, M. *Eur. Phys. J. D* **2002**, *20*, 243.
- (15) Manninen, K.; Akola, J.; Manninen, M. *Phys. Rev. B* **2003**, *68*, 235412.
- (16) Chuang, F.; Wang, C. Z.; Ho, K. H. *Phys. Rev. B* **2006**, *73*, 125431.
- (17) Wales, D. J.; et al. The Cambridge Cluster Database. <http://www-wales.ch.cam.ac.uk/CCD.html>.
- (18) Doye, J. P. K.; Wales, D. J. *J. Chem. Soc., Faraday Trans.* **1997**, *93*, 4233.
- (19) Doye, J. P. K.; Wales, D. J. *New J. Chem.* **1998**, *22*, 733.
- (20) Doye, J. P. K.; Wales, D. J. *Phys. Rev. Lett.* **2001**, *86*, 5719.
- (21) Doye, J. P. K. *Phys. Rev. B* **2003**, *68*, 195418.
- (22) Doye, J. P. K.; Hendy, S. C. *Eur. Phys. J. D* **2003**, *22*, 99.
- (23) Doye, J. P. K. *Comput. Mater. Sci.* **2006**, *35*, 227.
- (24) Soler, J. M.; et al. *J. Phys.: Condens. Matter* **2002**, *14*, 2745.
- (25) Hamann, D. R.; Schlüter, M.; Chiang, C. *Phys. Rev. Lett.* **1979**, *43*, 1494.
- (26) Kleinman, L.; Bylander, D. M. *Phys. Rev. Lett.* **1982**, *48*, 1425.
- (27) Anglada, E.; Soler, J. M.; Junquera, J.; Artacho, E. *Phys. Rev. B* **2002**, *66*, 205101.
- (28) Perdew, J. P.; Burke, K.; Ernzerhof, M. *Phys. Rev. Lett.* **1996**, *77*, 3865.
- (29) Näher, U.; Zimmermann, U.; Martin, T. P. *J. Chem. Phys.* **1993**, *99*, 2256.
- (30) Aguado, A.; Molina, L. M.; López, J. M.; Alonso, J. A. *Eur. Phys. J. D* **2001**, *15*, 221.
- (31) Aguado, A.; López, J. M. *Phys. Rev. Lett.* **2005**, *94*, 233401.
- (32) Aguado, A. *J. Phys. Chem. B* **2005**, *109*, 13043.
- (33) Baletto, F.; Ferrando, R. *Rev. Mod. Phys.* **2005**, *77*, 371.
- (34) Wales, D. J. *Energy Landscapes with Applications to Clusters, Biomolecules and Glasses*; Cambridge University: Cambridge, England, 2003.